Polarized Resonance Raman and FTIR Reflectance Spectroscopic Investigation of the Molecular Orientation in Industrial Poly(vinyl chloride) Specimens

G. A. Voyiatzis,* K. S. Andrikopoulos, and G. N. Papatheodorou

Foundation for Research and Technology-Hellas, Institute of Chemical Engineering and High Temperature Chemical Processes and Department of Chemical Engineering, University of Patras, P.O. Box 1414, GR-265 00 Patras, Greece

E. I. Kamitsos,* G. D. Chryssikos, and J. A. Kapoutsis

National Hellenic Research Foundation, Theoretical and Physical Chemistry Institute, 48 Vassileos Constantinou Avenue, GR-116 35 Athens, Greece

S. H. Anastasiadis[†] and G. Fytas

Foundation for Research and Technology-Hellas, Institute of Electronic Structure and Laser, P.O. Box 1527, GR-711 10 Heraklion Crete, Greece

Received October 22, 1999; Revised Manuscript Received April 24, 2000

ABSTRACT: The molecular orientation of uniaxially drawn commercial poly(vinyl chloride), PVC, specimens has been investigated by polarized Fourier transform infrared (FTIR) in the specular reflectance mode and by resonance Raman scattering in various combinations of sample orientation, scattering configuration and polarization geometry. The orientation was examined as a function of the specimen draw ratio. The Kramers−Kronig transformation has been used to obtain infrared absorption spectra from the FTIR reflectance data; the orientation was determined by the dichroic ratio of the C−Cl stretching and CH_2 rocking modes of PVC. The resonance Raman spectra of polyene segments that result from partial thermal degradation/dehydrochlorination of PVC during processing have been utilized in order to determine the parameters of the orientation distribution function. The all-trans conjugated polyene sequences formed during degradation are considered as rodlike segments in the polymer backbone and are used as indicators of orientation within the amorphous-like polymer phase. As far as the trends are concerned, data analysis showed good agreement between FTIR and Raman results regarding the induced molecular orientation in industrial PVC specimens.

I. Introduction

The orientation of the structural units in a solid polymer, as a result of various forming processes such as drawing and extrusion, may have a profound influence on the macroscopic physical properties of the material. Uncertainties in the uniformity of mechanical properties have revealed the necessity for a fast on line molecular orientation monitoring during industrial processing. Many investigations have been undertaken to characterize the orientation distribution of the macromolecular chains or segments of the chains or crystalline regions in the polymer.[1] The experimental techniques employed[1−22] to determine the molecular orientation of stretched polymers include birefringence measurements, infrared dichroism, polarized Raman scattering, fluorescence polarization, anisotropy of broadline NMR signals, X-ray diffraction, light scattering, small-angle neutron scattering, and sonic pulse propagation. All these techniques attempt to approximate the orientation distribution function, $f(\theta)$, which in the case of uniaxially drawn samples relates the number of entities lying in one direction with the angle they make with respect to the draw direction. This function is usually written in an expanded form as a series whose terms are Legendre polynomials.

Roe[23] had first formulated the expansion of $f(\theta)$, but the analysis of the Raman scattering spectrum of a material, yielding molecular orientation, dates back to the original work of Bower.[24] So far this method has been applied, at times in slightly modified versions, to a number of semicrystalline polymers.[3,11,18,21] Raman spectroscopy provides information on both the second ($\langle P_2(\cos\theta)\rangle = [3\langle\cos^2\theta\rangle - 1]/2$, θ being the orientation angle) and the fourth ($\langle P_4(\cos\theta)\rangle = [35\langle\cos^4\theta\rangle - 30\langle\cos^2\theta\rangle + 3]/8$) moments of the orientation distribution function, referred to as P_2 and P_4, respectively.[24,25] Both parameters are necessary to fully determine the orientation distribution function and understand the mechanical properties of oriented polymers in terms of molecular models. Infrared dichroism is directly related to the second-order term and has also been applied for measuring the orientation of polymer segments.[1,26,27] Raman[25] and infrared[26] spectra of semicrystalline polymers may provide information about the chains in the crystalline phase and certain chain conformations in the amorphous phase although, in most cases, quite poor X-ray diffraction pattern and small crystallite size do not facilitate a complete polymer microstructure analysis. Raman spectroscopy combined with FTIR in the reflectance mode constitutes a powerful tool for the investigation of thick samples without the need for microtoming, which might cause changes in the distribution of chain orientation. It is precisely the scope of this paper to demonstrate that these techniques can be

[†] Also at the Physics Department, University of Crete, P.O. Box 2208, GR − 710 03, Heraclion, Crete, Greece.

10.1021/ma991772m CCC: $19.00
Published on Web 07/06/2000

extended to the study of commercial stretched polymers of moderate crystallinity, like poly(vinyl chloride), and eventually proceed to the development of a fast characterization method that probes the molecular orientation of polymers in the production line, optimizing, on that account, the process parameters.

Raman scattering has already been used[28] in combination with birefringence measurements for the investigation of molecular orientation in macroscopically stretched PVC specimens; the study utilized the C−Cl stretching region of the Raman spectrum around 610−710 cm^{-1}, which, however, has been shown[29] to be composed of nine Lorentzian peaks attributed to vibrations in both the crystalline and amorphous regions. The Raman data for peaks at 608 and 638 cm^{-1}, attributed to the A_g and B_{3g} species vibrations in the crystalline phase, were analyzed to give $\langle P_2(\cos\theta)\rangle_{cryst}$ and $\langle P_4(\cos\theta)\rangle_{cryst}$ averaged over the distribution of orientations of the crystallites, where θ is the angle between the *c* axis of a typical crystallite and the draw direction. At the same time, the birefringence measurements provided information on the $\langle P_2(\cos\theta)\rangle_{all}$ of both crystalline and amorphous domains. However, it is known from different independent techniques that the structure of PVC is not regular since it contains conformational and configurational defects. The concentration of the latter may be so large that the actual structure of solid PVC could approach that of a disordered polymeric material. Indeed, Rubcic and Zerbi have applied[30,31] theoretical and numerical methods to understand the dynamics and vibrational (IR) spectra of PVC containing conformational and configurational disorder. On these grounds, they concluded that the complex chemical structure of PVC (conformation and stereospecificity) gives rise to a complicated and strongly overlapping pattern in the C−Cl stretching region; thus, only a suggestive character to band assignments can be obtained in this spectral region.[30,31]

Thermal degradation of PVC[32] has been shown to significantly alter[33−45] the Raman spectrum; new Raman bands appeared at about ∼1100 and ∼1500 cm^{-1} and were attributed to resonance Raman vibrations of conjugated polyene sequences, $(-CH{=}CH-)_n$, formed by the dehydrochlorination of PVC. The position of the peak at about 1500 cm^{-1} is directly related[41] to the length of the conjugated sequences, *n*, whereas the intensity of the resonance Raman band around 1100 cm^{-1} is related to the degree of degradation and the exciting radiation wavelength. It was found that it is possible to detect conjugated polyenes down to levels of 0.003%.[33,34]

Infrared dichroism in combination with birefringence, visible and ultraviolet dichroism was used long time ago[46] for the investigation of molecular orientation in macroscopically drawn poly(vinyl chloride) films; UV dichroism of polyene structures contained in dehydrochlorinated PVC samples was suggested as a useful means of evaluating the orientation of the PVC part of this polymer. More recently, polarized attenuated total reflection Fourier transform infrared dichroism (FTIR/ATR) was utilized to evaluate the surface orientation of poly(ethylene terephthalate),[22,47] of uniaxially stretched polypropylene sheets[48] as well as injection-molded plaques[49] or extrusion-molded sheets[50] of liquid crystalline polymers (LCP). Besides, polarized external reflectance infrared spectroscopy has already been used for measuring polymeric products orientation[51] and poly(ethylene terephthalate) surface orientation.[52,53] Moreover, polarized FTIR microspectroscopy has been applied to characterize the orientation in uniaxially drawn poly(ethylene terephthalate) film[54] and in extrusion-molded strands of a thermotropic LCP.[55]

In this paper, we present an investigation of the molecular orientation of uniaxially drawn industrial PVC specimens utilizing polarized resonance Raman scattering and FTIR dichroism in the reflectance geometry. Use of the Kramers−Kronig relation allows transformation of the FTIR reflectance measurements into absorption data. Infrared bands sensitive to specimen drawing were employed to tentatively evaluate the second moment of the orientation distribution function of this structurally disordered polymer. On the other hand, advantage is taken of the resonance Raman conditions that result from partial thermal degradation of PVC during specimen formation and drawing. The resonance Raman bands of the $(-CH{=}CH-)_n$ stretching modes, of the all-trans conjugated polyene sequences, are used in order to probe the orientation distribution function of the amorphous-like polymer phase. Analysis of the polarized Raman spectra leads to the determination of both the second and the fourth moments of the orientation distribution function. The P_2's extracted from both techniques are compared and discussed. The potential of the Raman method for use online during processing is also pointed out.

II. Experimental Section

Materials. The poly(vinyl chloride) drawn specimens were prepared by the R & D division of the A. G. Petzetakis S. A.−Hellenic Plastics and Rubber Industry, using commercial PVC (*K* value 65) and about 5% additives, such as stabilizers and lubricants, but no plasticizers. The compounding was done in a laboratory mixer of the company at 120−130 °C (dry blend) and 2500 rpm. The material was then calendered at 170−180 °C for 3−5 min and pressed into sheets of dimensions 17 × 17 cm^2 and a thickness of 3−5 mm. Specimens taken from these sheets were then drawn at 120 °C to the required draw ratio, λ, and were kept stretched for 15 min before quenching in a water bath at 15 °C for 10 min. The experimental vibrational spectra were not corrected for the additives because of their relatively small concentration. In any case, the FTIR and Raman spectra of all additives were measured and found to exhibit no bands at frequencies that may interfere with the vibrational modes used as probes for data evaluation.

Laser Raman Scattering. Raman spectra have been measured in the micro-Raman backscattering geometry. For comparison, representative measurements have been also conducted using the 90° Raman scattering configuration. The experimental setup as well as the polarization geometries used for obtaining polarized Raman spectra in the 90° scattering geometry has been described previously.[19]

The Raman spectra were excited with the linearly polarized 514.5 nm line of an air-cooled Ar^+ laser (Spectra-Physics 163-A42). A narrow-band-pass interference filter was used for the elimination of the laser plasma lines. The excitation beam was directed to the sample compartment of a properly modulated metallurgical microscope (Olympus BHSM-BH2). The microscope was used for the delivery of the excitation laser beam on the sample and the collection of the backscattered light through a beam splitter and the objective lens adapted to the aperture of the microscope. The focusing objective was a Long Working distance (8 mm) 50×/0.55 Olympus lens. The spectra were obtained using a ∼2 mW laser power on the specimen for a total integration time of 30 s. A viewing screen connected to the microscope offered good sample positioning and beam focusing as well as direct surface inspection. The Raman-scattered radiation was focused on the slit of a single monochromator after being passed through a notch holographic

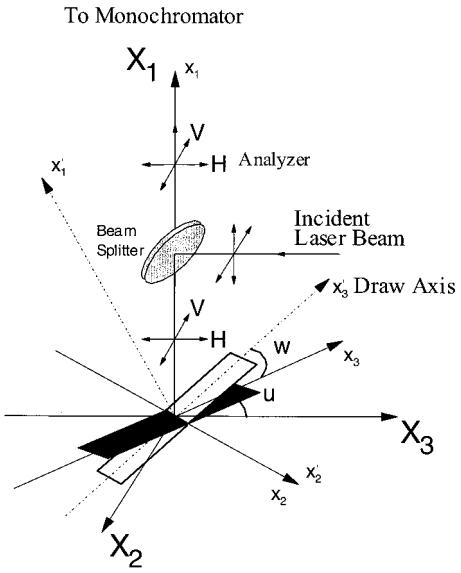

Figure 1. Coordinate axes for the Raman backscattering configuration (see text for details).

filter (HFN-514−1.0 of Kaiser Optical Systems, Inc.) for the elastic Rayleigh scattering rejection. The Raman system employed was the T-64000 model of Jobin Yvon (ISA−Horiba group). Dispersion and detection of the Raman photons were done by an 1800-grooves/mm grating and a 2D CCD detector (operating at 140 K), respectively. The spectral slit width was approximately 8 cm^{-1}. The incident beam polarization was selected by an optical rotator (90°). A dichroic sheet polarizer analyzed the scattered radiation, and a half-wave plate was used after the polarizer whenever needed in order to ensure the same maximum polarization response from the grating. All spectra were corrected taking into account the beam splitter's response in polarization of incident and scattered radiation. The total response of the system was checked using CCl_4 as reference. The Raman spectra shown in the next Section were obtained using the laser Raman microscope, because this technique yields accurate intensity data with significantly reduced noise, compared to conventional polarized Raman measurements at a 90° scattering geometry. The backscattering geometry used in this study is depicted in Figure 1. Two sets of coordinate axes are fixed; one refers to the sample, $Ox_1x_2x_3$ (or $Ox_1'x_2'x_3'$, when the sample is tilted by an angle w), and the second to the experimental setup, $OX_1X_2X_3$. The notation of Raman polarization measurements comprises a combination of three letters, like *h*-VV. The small letter in italics (*h*, *v*, *d*, or *s*) denotes the orientation of the draw axis, Ox_3 ($w = 0°$) or Ox_3' ($w \neq 0°$), relative to the laboratory fixed coordinates, $OX_1X_2X_3$; *h*, when aligned along the OX_3 axis ($u = 0°$ and $w = 0°$); *v*, when aligned along the OX_2 axis ($u = 90°$ and $w = 0°$); *d*, when aligned at the bisector of the X_3OX_2 angle ($u = 45°$ and $w = 0°$); and *s*, when aligned along the OX_1 axis ($w = 90°$). The two capital letters (HH, HV, VV, or VH) denote the polarization direction of the excitation and scattered light, respectively; H, when the polarization is parallel to the OX_3 axis, and V, when the polarization is parallel to the OX_2 axis.

FTIR Specular Reflectance Measurements. This technique was used as an independent probe of the molecular orientation, for comparison with the data obtained by Raman spectroscopy. The industrial PVC specimens were thick (3−5 mm), and, therefore infrared spectra could not be measured by the transmission mode which is usually employed in polymer studies. As an alternative, reflectance measurements were performed in order to avoid microtoming the samples and thus perturbing the molecular orientation.

Infrared spectra were measured in the specular reflectance mode on a Bruker vacuum spectrometer (IFS 113v) equipped with a near-normal incidence (11°) reflectance accessory. A KRS-5 wire grid polarizer was positioned before the sample

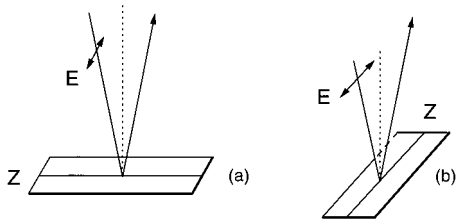

Figure 2. Coordinate system for infrared reflectance measurements. The draw direction of the PVC specimen is indicated by *Z*. The incident light is polarized perpendicular to the plane of incidence, with the vector of the electric field being perpendicular to *Z* (a) or parallel to *Z* (b). The angle of incidence is 11°.

to polarize the infrared radiation perpendicular to the plane of incidence. The polarizer remained fixed and the sample was rotated by 90° to obtain reflectance spectra with different polarization directions. The coordinate system employed for polarized specular reflectance measurements is shown schematically in Figure 2. The reflectance spectrum of a high reflectivity aluminum mirror was measured with the polarizer in place and the same instrument settings and used as reference spectrum. All spectra were measured at room temperature and represent the average of 200 scans at 2 cm^{-1} resolution.

The analysis of the specular reflectance data was performed using the Kramers−Kronig inversion technique. The Bruker HIL program was utilized in order to perform the Kramers−Kronig transformation on the PVC data, while the required extrapolation of the reflectance data outside of the range of measurements ($\nu \rightarrow 0$, $\nu \rightarrow \infty$) was done using the Bruker EXTPOL program.[56]

It should be noted that the reflectance spectrum is more sensitive to the behavior of the top surface of the polymer specimen. The amplitude of radiation, which propagates into the polymer sheet, decreases strongly in the regions of absorption. The penetration depth for the infrared beam may be estimated as the inverse of the adsorption coefficient $\alpha(\nu)$.[26] It will become evident in the Results section that for the studied PVC specimens $\alpha(\nu)$ is on the order of 5×10^2 cm^{-1} in the C−Cl stretching region and, therefore, the penetration depth is on the order of 20 μm. Thus, the orientation function obtained from the infrared data may be well regarded as representing the bulk orientation, since one should not expect surface effects to persist down to thickness larger than a few molecular dimensions.

III. Results

A. Raman Scattering Measurements. In Figure 3, three Raman spectra of PVC samples are presented; the Raman spectrum of the commercial PVC powder used for the preparation of the drawn specimen, the Raman spectrum of an isotropic, $\lambda = 1$, PVC sample obtained from the industrial master batch, and the Raman spectrum of a uniaxially stretched at $\lambda = 2.24$ industrial PVC sample obtained with parallel to draw axis polarization geometry, *v*-VV. In the spectral window of the PVC powder given here, the main vibrational features are: (i) the low-frequency band structure at 600−700 cm^{-1} assigned to C−Cl stretching of different PVC conformations, (ii) the CH_2 twist−CH_2 wag vibrational modes at around 1335 cm^{-1}, and (iii) the CH_2 bending at 1432 cm^{-1}. In the Raman spectrum of the industrial PVC sample measured before stretching two new vibrational bands appeared at around 1127 and 1515 cm^{-1}. These new Raman bands are attributed to stretching vibrations of conjugated double bonds formed in industrial PVC specimens by partial thermal degradation, as already referred to in the Introduction. The intensity of these new bands is comparable or even

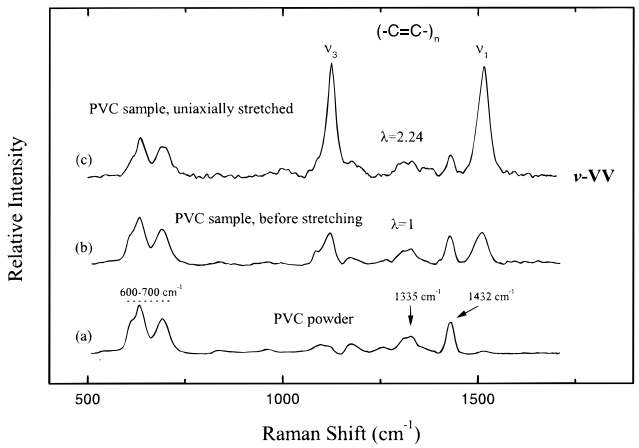

Figure 3. Micro-Raman spectra of PVC powder (a), of PVC industrial sample before stretching (b), and of a uniaxially stretched PVC industrial sample measured in the *v*-VV configuration (c). The spectra are shifted along the intensity axis for clarity of presentation.

higher than those of internal PVC bands, because of the resonance Raman enhancement exhibited by the polyene normal modes with excitation in the visible. Moreover, the intensity of the polyene bands is strongly influenced by the polarization of the incident and scattered radiation. This is demonstrated clearly in the polarized (*v*-VV) top spectrum of Figure 3 for the uniaxially drawn PVC sample; the band intensities of the skeletal $(-C{=}C-)_n$ stretching modes are highly enhanced in the parallel to the draw axis, and hence to the direction that the polymer backbone tends to orient, polarization geometry *v*-VV. It is precisely the aim of the present work to probe the molecular orientation of stretched PVC industrial samples by means of the orientation of the conjugated polyene segments.

In Figure 4 typical polarized Raman spectra are depicted of industrial PVC samples before and after uniaxial drawing, using two polarization geometries. The characteristic band structures exhibiting different dependence on the drawing process are noted; the C−Cl stretching in low-frequency region, the CH_2 bending at 1432 cm^{-1}, and the stretching of conjugated double bonds at 1127 and 1515 cm^{-1}. Before drawing, there is no preferred orientation since the sample is essentially isotropic at a molecular level; thus no differences are found between VV and HH scattering intensities for all spectral features (Figure 4a). However, when the sample is stretched (Figure 4b) the VV and HH spectra develop differences in relative band intensities. The extent of such differences depends on the position of the sample, *v* or *h*, with respect to the laboratory-fixed coordinates (see Figure 1), and reflects the anisotropy induced by the drawing process. The intensity of the C−Cl band, which is almost perpendicular to the polymer chain axis, is enhanced in the polarization geometries which are perpendicular to the specimen orientation and, hence, to the draw axis, *v*-HH and *h*-VV. To the contrary, the bands of the skeletal polyene stretching modes are highly enhanced in the parallel polarization geometry to the drawing direction, *v*-VV and *h*-HH. It is of interest to notice also the behavior of the CH_2 bending vibration; the scattering intensity of this PVC internal mode seems to remain unaffected by polarization of radiation and sample orientation geometry, suggesting a minimal sensitivity to induced molecular orientation.

In Figure 5, *h*-HH and *h*-VV polarized spectra are shown for industrial PVC samples drawn at various draw ratios. To facilitate comparison, the spectra have been normalized so that the intensity of the 1515 cm^{-1} band is the same in all *h*-HH spectra. In this way, the intensity of the 1515 cm^{-1} band in the crossed polarized spectra, *h*-VV, demonstrates a clear decrease upon increasing macroscopic draw ratio, implying an analogous increase in the molecular orientation. The second intense polyene band at 1127 cm^{-1} exhibits the same behavior. In the same figure, we can observe that the intensity of CH_2 bending mode at ∼1432 cm^{-1} remains practically independent of draw ratio and polarization geometry. Also, the relative intensity of the C−Cl band at ∼650 cm^{-1} in the *h*-HH spectra shows a gradual decrease upon increasing draw ratio.

The behavior of the Raman bands discussed above is presented in Figure 6 in terms of the polarization ratio, *h*-HH/*h*-VV, vs draw ratio, λ. It is apparent that the polarization ratio of the CH_2 bending mode is almost independent of λ, while that of the C−Cl stretching mode shows a weak dependence on draw ratio. The *h*-HH/*h*-VV ratio for the 1515 cm^{-1} band of conjugated double bond segments is strongly influenced by λ, revealing its pronounced sensitivity to drawing-induced molecular orientation. Therefore, the stretching vibrational modes of the skeletal double bonds can be employed to probe molecular orientation in uniaxially drawn industrial PVC samples.

B. Infrared Dichroism and Orientation Function. As already mentioned, polarized infrared measurements may be used to investigate molecular orientation in polymeric materials. This is due to the fact that the infrared absorption of a characteristic group of the polymer is given by

$$A \propto [(\partial \boldsymbol{\mu}/\partial r)\cdot \mathbf{E}]^2 = [(\partial \mu/\partial r)E]^2 \cos^2\gamma \qquad (1)$$

where $\partial\boldsymbol{\mu}/\partial r$ is the transition dipole moment, **E** is the electric field of the infrared radiation, and γ is the angle between the dipole moment and the electric field. It is evident that maximum absorption is obtained when the radiation is polarized parallel to the dipole moment that develops during the vibration of a characteristic group, while no absorption will be measured for (absolutely) perpendicular polarization. For a random distribution of orientations of the absorbing group and, therefore, random orientation of the resulting dipole moments, the measured infrared absorption will be independent of polarization, whereas, when there is partial alignment the absorption will depend on the polarization of the infrared radiation. Therefore, by using linearly polarized infrared light the orientation of the functional groups of a polymer can be investigated.

The absorption anisotropy is expressed by the dichroic ratio, *D*, defined as, $D = A_{\parallel}/A_{\perp}$, where $A_{\parallel}$ and $A_{\perp}$ are the absorptions measured with the incident radiation being polarized parallel and perpendicular, respectively, to a reference direction. For the case of polymers, the reference direction is usually the draw direction. In the present study the absorption, A, is replaced by the absorption coefficient, $\alpha(\nu)$, calculated by means of eq 2

$$\alpha(\nu) = 4\pi\nu k(\nu) \qquad (2)$$

where $k(\nu)$ is the extinction coefficient spectrum calculated from the Kramers−Kronig analysis of the specular

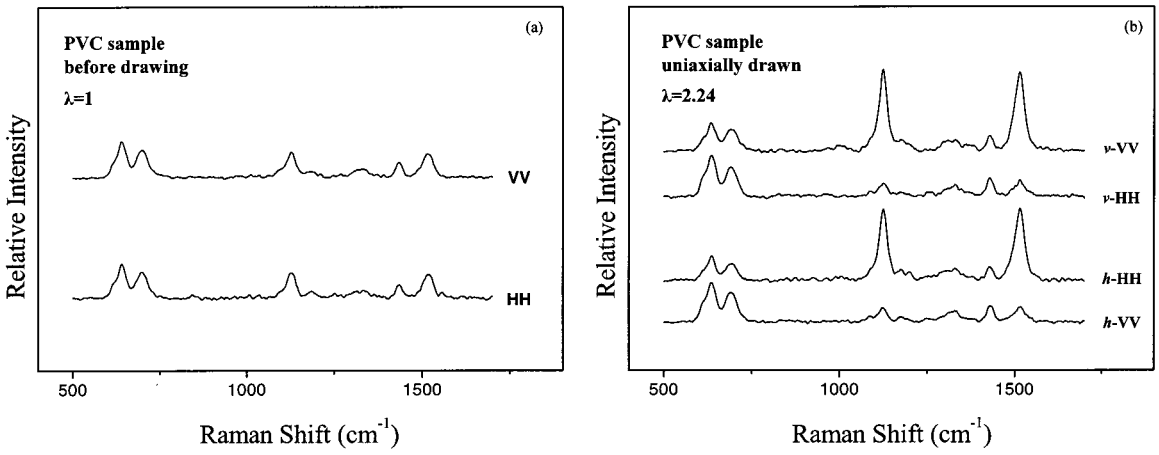

Figure 4. Micro-Raman spectra of a PVC industrial samples before (a) and after (b) uniaxial drawing, measured in two different polarization configurations. The spectra are shifted vertically for clarity.

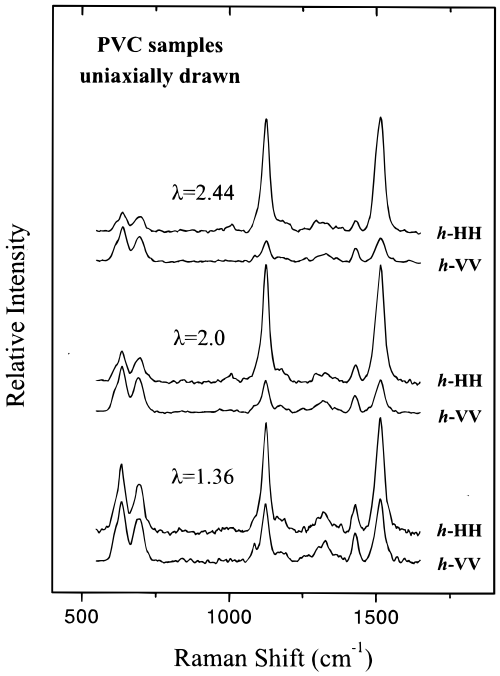

Figure 5. Polarized *h*-HH and *h*-VV micro-Raman spectra of industrial PVC samples uniaxially stretched at different draw ratios. Spectra are displaced along the vertical axis to allow comparison.

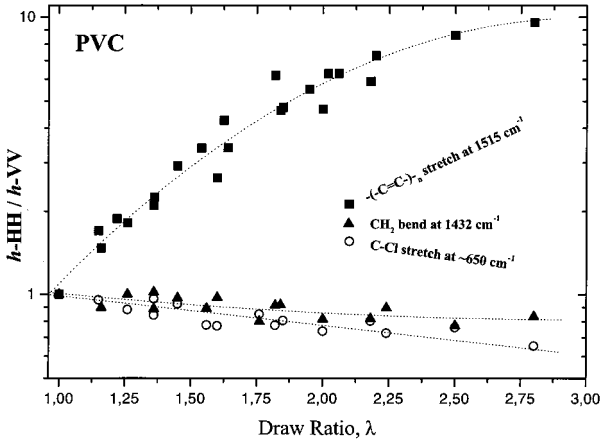

Figure 6. Polarization ratio, *h*-HH/*h*-VV, vs draw ratio, λ, for uniaxially drawn PVC specimens. Data are shown for the CH_2 bending, C−Cl stretching, and $(-C{=}C-)_n$ stretching modes.

reflectance spectrum[56] and the frequency ν is given in wavenumbers (cm^{-1}).

For uniaxially oriented polymers the orientation of a polymer chain can be described by the orientation function $f(\theta)$, where θ is the angle between the stretching direction and the axis of the polymer chain. If it is assumed that the distribution of polymer chains is random in the plane perpendicular to the stretching direction, then the distribution function can be written in a series of Legendre polynomials.[57] The average of the second-order Legendre polynomial, $\langle P_2(\cos\theta)\rangle$, is known as the Hermans−Stein orientation function of polymer chains and can be calculated from dichroic measurements by the relationship[58−60]

$$\langle P_2(\cos\theta)\rangle = [3\langle\cos^2\theta\rangle - 1]/2 = [(D-1)(D_o+2)]/[(D+2)(D_o-1)] \quad (3)$$

where $D_o = 2\cot^2\psi$ is the dichroic ratio for perfect orientation, with ψ being the angle between the direction of the vibrational transition moment and the polymer chain axis. A value of 1 for $\langle P_2(\cos\theta)\rangle$ represents perfect orientation of the chain axes parallel to the draw direction, a value of zero is obtained when the chains are randomly oriented and a value of $-1/2$ represents perfect orientation of chains perpendicular to the draw direction. For vibrations for which $\psi = 90°$, eq 3 reduces to

$$\langle P_2(\cos\theta)\rangle = 2(1-D)/(D+2) \quad (4)$$

while for $\psi = 0°$ one obtains

$$\langle P_2(\cos\theta)\rangle = (D-1)/(D+2) \quad (5)$$

Therefore, the second moment of the orientation function can be calculated directly from polarized infrared measurements.

IV. Analysis and Discussion

A. Analysis of Raman Spectra. On the basis of the above Raman data, we present in this section an approach for the quantification of molecular orientation in uniaxially drawn industrial PVC samples, utilizing the polarization characteristics of the skeletal double bond stretching mode at 1515 cm^{-1}.

Systems containing extended polyene $(-CH{=}CH-)_n$ sequences have been studied in great detail especially

in the last 20 years; they include polyacetylene (pristine or doped),[61] β-carotene,[62] and degraded poly(vinyl chloride).[33−45] Conjugated double bonds have a very simple Raman spectrum. The two main bands observed are highly enhanced due to resonance Raman effect and electron−phonon coupling.[63] On that account, it is estimated that Raman scattering can detect conjugated double bonds in extremely low concentrations.[33,34] Parker et al.[62] has studied recently the Raman spectrum of β-carotene using excitation wavelengths from visible to near-infrared. The Raman spectrum appeared[62] independent of excitation wavelength, although the intensities of overtones and combinations of the ν_{C-C} and $\nu_{C=C}$ fundamentals varied strongly, and the UV/vis/NIR spectrum showed no allowed electronic transitions from the ground state beyond ~750 nm. This result has provided strong support for the existence of a different to resonance Raman mechanism for the enhancement of bands of extended polyene $(-CH=CH-)_n$ sequences, with $n > 10$. Furthermore, resonance Raman measurements[34a] with 488, 514.5, and 568 nm excitation on several degraded PVC samples, containing conjugated polyene sequences at concentration levels of ca. 0.1%, gave spectra with strong ν_{C-C} and $\nu_{C=C}$ peaks. However, these two peaks were not detectable when the 647.1 nm excitation was used. The major part of this dramatic intensity drop was ascribed[62] as the result of moving from the wavelength regime where resonance Raman enhancement occurs to the one where only the π-electron/phonon coupling is operative. It was therefore concluded[62] that excitation in the visible leads to resonance Raman enhancement, which is some 2 orders of magnitude stronger than the effect of the π-electron/phonon coupling mechanism.

Using an excitation laser line at 514.5 nm, resonance Raman conditions are fulfilled mainly for a range of conjugation lengths of $n \approx 10-13$. In typically degraded PVC, a distribution of conjugated sequence lengths is present that contains polyenes of 10−13 double bonds as well. In present work, with green laser line excitation, this narrow range of sequence length gives rise to strong Raman peaks at around 1127 and 1515 cm^{-1}. Therefore, we use these two Raman frequencies that represent a narrow dispersion of conjugated double bonds to quantify the drawn-induced molecular orientation in industrial PVC samples. All-trans polyenes are formed mainly in the amorphous part of the polymeric sample and they are rodlike.[63] Cis polyenes are not stable, especially at temperatures as high as 100 °C used in industrial processing or in thermal treatment of PVC.[63] As a consequence, the all-trans polyenes formed by thermal degradation of PVC in the polymer backbone will characterize the orientation of the amorphous areas in the sample.

In this work the analysis of Pigeon et al.[9] is adopted, which is based on the theory of Bower[24] for the determination of the distribution of molecular orientation in oriented polymers, and use polarized micro-Raman spectroscopy in the backscattering configuration. The total Raman scattering intensity is given by

$$I_s = I_o \sum (\sum I_i I'_j a_{ij})^2 \tag{6}$$

where a_{ij} are all components of the Raman tensor for the vibrational mode studied, I_i and I_j' are the polarization directions of the incident and scattered light with respect to the set of axes fixed in the sample, and I_o is a constant depending on incident light intensity and instrumental factors. The experimental values are of the form $I_o \sum a_{ij} a_{pq}$, and in the case of uniaxial statistical symmetry with no preferred orientation one can write

$$\sum a_{ij} a_{pq} = 4\pi^2 N_o \sum M_{l00} A_{l00}^{\ ijpq} \tag{7}$$

M_{l00} is expressed in terms of Legendre polynomials, $M_{l00} = (1/4\pi^2)\{(2\lambda + 1)/2\}^{1/2} \langle P_l(\cos\theta)\rangle$ ($l = 0, 2, 4$), and $A_{l00}^{\ ijpq}$ is a sum containing a_1, a_2, a_3. There are only five independent nonzero sums $\sum a_{ij} a_{pq}$ that are of the form $\sum a_{ii} a_{jj}$ and $\sum a_{ij}^2$, in agreement with the analysis of Mead.[64] These are

$$\sum a_{22}^{\ 2} = xR_1 + yR_2 + 3zR_3 = I_{h-VV}\ (w = 0°,\ u = 0°) \tag{8a}$$

$$\sum a_{33}^{\ 2} = xR_1 - 2yR_2 + 8zR_3 = I_{h-HH}\ (w = 0°,\ u = 0°) \tag{8b}$$

$$\sum a_{32}^{\ 2} = xR_4 - yR_5 - 4zR_3 = I_{h-HV}\ (w = 0°,\ u = 0°) \tag{8c}$$

$$\sum a_{22} a_{33} = xR_6 - yR_7 - 4zR_3 = \frac{I_{h-VV}\ (w = 0°,\ u = 0°)}{2} + \frac{I_{h-HH}\ (w = 0°,\ u = 0°)}{2} - 2I_{d-HV}\ (w = 0°,\ u = 45°) \tag{8d}$$

$$\sum a_{12}^{\ 2} = xR_4 + 2yR_5 + zR_3 = I_{s-HV}\ (w = 90°) \tag{8e}$$

Each nonzero sum is correlated to a specific polarization geometry (or combination of geometries) as has been already designated in the Experimental Section.

In the above equations, I_{ij} is the experimentally observed intensity of the scattered light, when the incident light is polarized parallel to the i axis and the scattered light is polarized parallel to the j axis, fixed to the laboratory coordinates; R_i are second-order polynomials of a_1/a_3 and a_2/a_3; $x = b$ (an experimental constant including the a_3 element of the diagonalized Raman tensor); $y = \langle P_2(\cos\theta)\rangle b$; and $z = \langle P_4(\cos\theta)\rangle b$. Hence, in the above five equations (8a−e) there are five unknowns: a_1, a_2, x, y, and z. Furthermore, it was preferred not to use eq 8e to avoid microtoming the samples and eventually perturbing the molecular orientation. Of course, another geometry could have been used with different values of the w angle, but that would increase the number of geometries needed and introduce errors due to birefringence effects (because of the tilting of the sample), as well as to bad focusing on the sample. Nevertheless, ab initio calculations, which have been performed on prototype molecules to derive the terms of Raman tensor of conjugated double bonds, showed[63] that the main term of the Raman scattering tensor is the a_{33} element parallel to the all-trans chain. The a_{32}, a_{23}, a_{22}, and a_{11} terms have a minor value. The domination of the a_{33} element becomes even stronger when the conjugation length increases. One can, thus, approximate the Raman tensor in resonance conditions with a symmetric one with cylindrical symmetry, i.e., the elements a_1 and a_2 of the diagonalized Raman tensor are considered equal and $a = a_1/a_3 = a_2/a_3$. The analytical expressions of the second-order polynomials, R_i, of α have been previously described,[21] while with the

assumption of a cylindrical Raman tensor the number of unknowns are now reduced to four.

The four remaining equations with four unknowns form a linear algebraic system. However, to further avoid use of eq 8d, which is also affected by birefringence effects, use is made of an equation resulting from the hypothesis of cylindrical Raman tensor, which relates α to the isotropic depolarization ratio, $\rho = (1 + \alpha^2 - 2\alpha)/(3 + 8\alpha^2 + 4\alpha)$, experimentally measured for the isotropic (unstretched) sample as $\rho = I_{HV}/I_{VV}$.[3,28]

Having calculated α, to determine the rest of the unknowns one then needs the three equations (8a−c) accurately modified as below:

$$I_{h-VV} = b\left[\frac{1}{15}(8\alpha^2 + 4\alpha + 3) + \frac{2}{21}(4\alpha^2 - \alpha - 3)\langle P_2(\cos\theta)\rangle + \frac{3}{35}(\alpha^2 - 2\alpha + 1)\langle P_4(\cos\theta)\rangle\right] \quad (9a)$$

$$I_{h-HH} = b\left[\frac{1}{15}(8\alpha^2 + 4\alpha + 3) - \frac{4}{21}(4\alpha^2 - \alpha - 3)\langle P_2(\cos\theta)\rangle + \frac{8}{35}(\alpha^2 - 2\alpha + 1)\langle P_4(\cos\theta)\rangle\right] \quad (9b)$$

$$I_{h-HV} = b\left[\frac{1}{15}(\alpha^2 - 2\alpha + 1) - \frac{1}{21}(-\alpha^2 + 2\alpha - 1)\langle P_2(\cos\theta)\rangle - \frac{4}{35}(\alpha^2 - 2\alpha + 1)\langle P_4(\cos\theta)\rangle\right] \quad (9c)$$

This system can be easily solved analytically. It is noted that measurements of ρ at different u angles (at $w = 0°$; see Figure 1), and at different sample locations confirmed that the unstretched sample is indeed isotropic. For an unstretched bulk PVC sample, $\rho \sim 0.45$, while for an unstretched PVC sample dissolved in THF, $\rho \sim 0.33$. In the first case we have approximated the Raman tensor with a cylindrical one. If we assume a molecular scattering tensor with only the a_{33} component being nonzero ($\rho = 0.33$), the above three equations are simplified ($\alpha = 0$) in agreement with Everall et al.[65]

A few PVC industrial samples were also studied in the 90° scattering configuration, and the corresponding orientation parameters were determined as before.[19]

B. Infrared Data Analysis. Polarized specular reflectance spectra of uniaxially drawn industrial PVC specimens are shown in Figure 7 for representative values of the draw ratio: $\lambda = 1.0$, 2.0, and 3.1. The polarized spectra obtained for $\lambda = 1.0$ are almost identical; increasing λ, however, results in pronounced differences between the spectra measured with polarizations perpendicular and parallel to the stretching direction. In particular, the perpendicular polarization appears to lead to larger reflectivity values.

Such differences due to polarization are evident also in the absorption coefficient spectra calculated by the Kramers−Kronig procedure. Such spectra are depicted in Figure 8 for the specimens whose reflectance spectra were given in Figure 7. It is evident that the spectral regions 580−720, 900−1000, 1220−1285, and 1300−1350 cm^{-1} are most sensitive to polarization of the incident radiation, in agreement with previous transmission studies of PVC thin films.[64−70] Bands in these regions have been assigned to C−Cl stretching, CH_2 rocking, CH_2 bending, and CH_2 wagging modes, respectively.[64,71] In the present investigation the 580−720 cm^{-1} C−Cl stretching region is being utilized, which can be deconvoluted into eight or 10 Lorentzian peaks

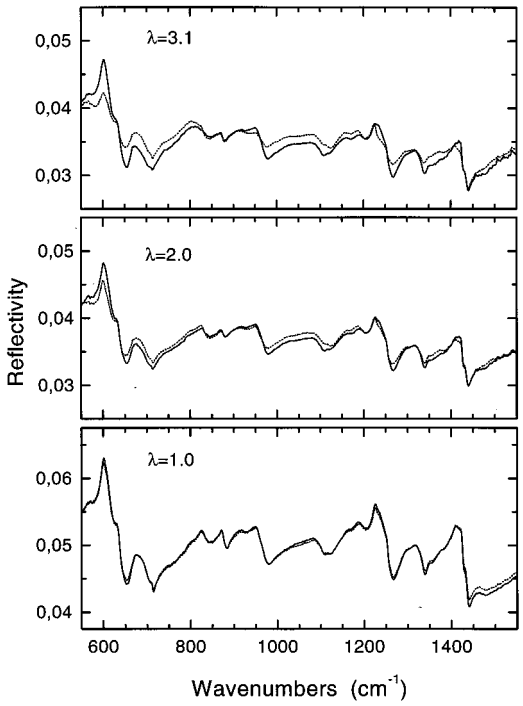

Figure 7. Representative polarized specular reflectance spectra of industrial PVC samples with draw ratios $\lambda = 1.0$, 2.0, and 3.1. Dotted spectra (...) were measured with polarization vector parallel to draw direction (see Figure 2a) and continuous line spectra (—) were measured with polarization vector perpendicular to draw direction (see Figure 2b).

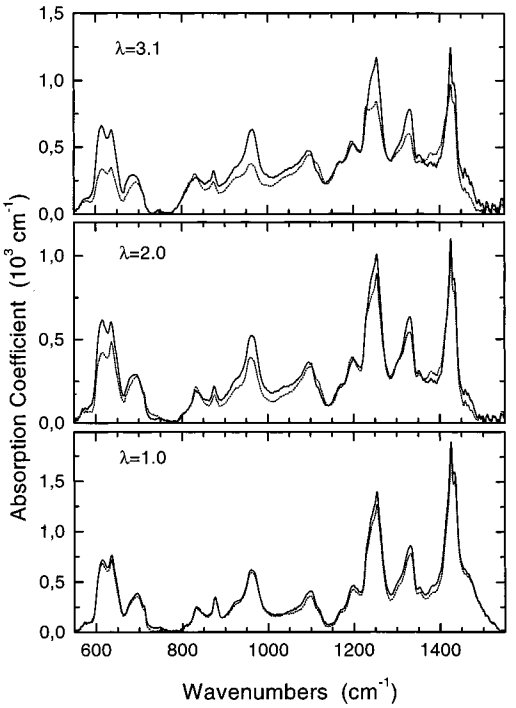

Figure 8. Polarized absorption coefficient spectra of PVC samples with draw ratios $\lambda = 1.0$, 2.0 and 3.1, calculated by Kramers−Kronig analysis of the measured specular reflectance spectra. Polarization conditions are defined as in Figure 7.

according to previous infrared[67,68,70] and Raman[72,73] studies. Table 1 lists the position of the infrared peaks found in previous works, with some of the proposed assignments.

For the deconvolution of the C−Cl stretching envelope of the industrial PVC specimens investigated in this

Table 1. Assignments of Infrared Absorption Bands (in cm^{-1}) of PVC in the C−Cl Stretching Region, 600−720 cm^{-1}, with Bands Numbered According to the Deconvolution Shown in Figure 9

band no.	IR band present study	ref 70	ref 68	ref 67	config[72]	conform[68]
1	604	607	605	603	S[a]	TTTT long trans seq
2	613	613	614	613	S	TT short trans seq
3	623	622	623	624	I	TGTTG′T
4	633	632	635	633	S	
5	639	639	638	639	S	TTTT
6	648	648	647	647	H	TTTG
7	680	677	681	677	I or H	TTG′G′
		689			H	
8	695	697	698	695	I	TGTG
9	708	706			H	

[a] Key: S, syndiotactic triad; I, isotactic triad; H, heterotactic triad.

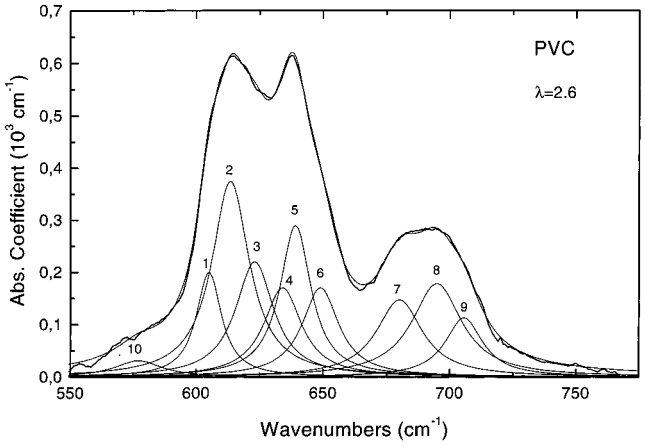

Figure 9. Example of curve fitting of the C−Cl stretching region of the absorption coefficient spectrum of a PVC sample (perpendicular polarization of sample with draw ratio $\lambda = 2.6$). The observed spectrum (thick line) was deconvoluted into 10 Lorentzian peaks. The thinner line shows the simulated spectrum. For details, see text.

work we followed the procedure outlined by Karacan et al.[70] The parallel and perpendicular polarized absorption spectra were deconvoluted independently using the positions and widths of peaks found in earlier studies[67,68,70] as starting values. These values were then allowed to change freely to obtain best fits. The peak positions and widths obtained for all spectra were averaged, and the spectra were refitted by fixing the positions and widths at these average values and allowing only the peak intensities to vary. It was found that nine Lorentzian peaks result in good fits of the C−Cl envelope. The position of the peaks found in this work are also given in Table 1 for comparison with the results of earlier infrared studies and lead to a quite satisfactory agreement. An example of deconvolution is shown in Figure 9 for the perpendicularly polarized spectrum of the $\lambda = 2.6$ specimen. An additional weak component at 575 cm^{-1} was also considered to improve the fit at the lower frequency tail of the C−Cl region.

The stronger peaks at 613 and 639 cm^{-1} have been assigned to the C−Cl stretching vibration of syndiotactic chain segments in amorphous and crystalline regions, respectively.[66,68,73] The dependence of the dichroic ratio D on draw ratio λ is shown in Figure 10 for the 613 and 639 cm^{-1} deconvoluted bands. For both bands, D decreases upon increasing λ. Since the dipole moment for the C−Cl stretching vibration is directed perpendicular to the polymer chain backbone,[66,70] the decrease of D is indicative of molecular orientation of the polymer chains along the stretching direction. Assuming that $\psi = 90°$, eq 4 can be used to calculate the second-order Legendre polynomial, $\langle P_2(\cos\theta)\rangle$, of the orientation distribution of PVC chains.

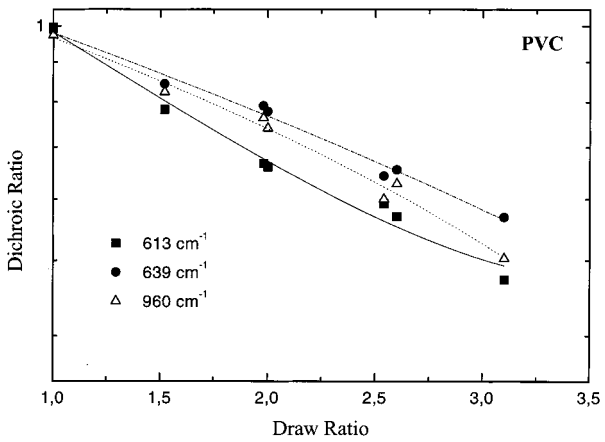

Figure 10. Dichroic ratios, D, for the 613, 639, and 960 cm^{-1} infrared peaks of PVC as a function of the macroscopic draw ratio, λ. Lines are drawn to guide the eye.

It is noted at this point that Rubcic and Zerbi[31] have concluded that heat or pressure treatments of PVC samples affect the vibrational spectra and give rise to overlapping bands, like the ones in the C−Cl stretching region. This appears to happen even when model PVC samples obtained by different polymerization conditions were used to deconvolute the C−Cl infrared region. Thus, the authors have attempted a new assignment of the C−Cl spectral region by considering the dymanics of conformationally/configurationally disordered PVC and applying a numerical method which associates density of states peaks with particular segments or islands of defects in an otherwise regular host lattice. They concluded that the envelope of the C−Cl infrared absorption originates from configurational and conformational irregularities whose contributions depend on their population and distribution throughout the polymer chain.

Considering the above points, and in order to provide a means for comparison of the infrared and Raman molecular orientation data for the PVC specimens studied in this work, we have averaged the orientational parameters from the more intense 613 and 639 cm^{-1} bands. In addition, we associate this orientation behavior in the C−Cl stretching region with that of syndiotactic segments of the chain backbone of PVC (Table 1).

Besides the C−Cl stretching modes, the CH_2 rocking motion active at 960 cm^{-1} has an induced dipole moment also perpendicular to the polymer chain.[66] It has been suggested that this band is composed of two components; one at 957 cm^{-1} (ordered regions) and the other at 970 cm^{-1} (disordered regions).[66] Deconvolution of the 960 cm^{-1} band has not been attempted here due to the complex background of the 900−1000 cm^{-1} envelope. As an alternative, we can employ the baseline approach of Jabarin[69] to obtain the dichroic ratio, D, for the 960 cm^{-1} envelope. The results for this band are also shown in Figure 10 vs draw ratio.

C. Evaluation of Molecular Orientation. A compilation of the orientation data resulted from the analysis of polarized Raman and FTIR spectra of the

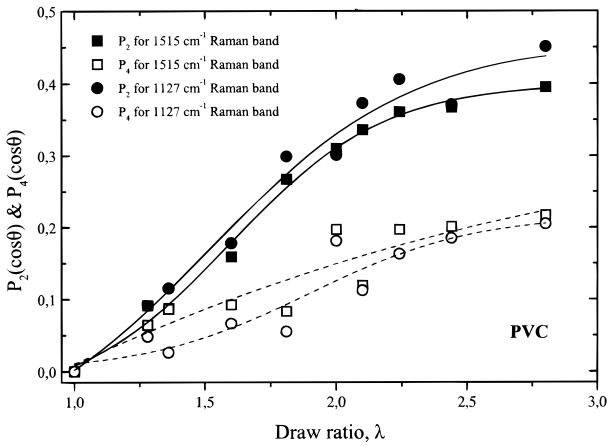

Figure 11. Second, P_2, and fourth, P_4, moments of the orientation distribution function of PVC, determined from the 1127 and 1515 cm^{-1} Raman bands of conjugated double bonds in backscattering configuration assuming a cylindrical tensor, as a function of the draw ratio. Lines are drawn to guide the eye.

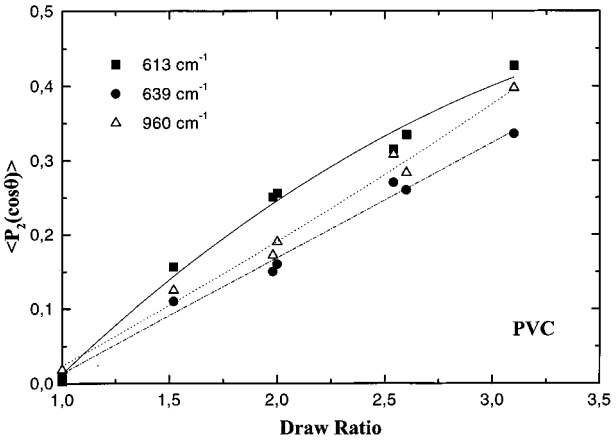

Figure 12. Second-order Legendre polynomial, $\langle P_2(\cos\theta)\rangle$, for the infrared peaks at 613, 639, and 960 cm^{-1} vs draw ratio, λ. Lines are drawn to guide the eye.

studied PVC industrial samples is presented in Figures 11 and 12, respectively. In both cases, increasing draw ratio, an enhancement of the second orientational moment, P_2, occurs. Although a rigorous analysis of orientation cannot be made by just measuring the *h*-HH and *h*-VV Raman spectra, it is evident that the obtained dependence of P_2 on draw ratio is consistent with the trends of the experimentally derived polarization ratio, *h*-HH/*h*-VV, and dichroic ratio, $A_\parallel/A_\perp$. This suggests that the present Raman analysis, assuming uniaxially symmetry of the drawn material and cylindrical symmetry of the Raman polarizability tensor, should be considered as unambiguous. The corresponding P_4 values that are also shown in Figure 11 vs draw ratio exhibit similar to P_2 trends, which follow the qualitative tendencies suggested for conjugated double bond segments by Figure 6. It should be noted that the values of P_4 fall within the acceptable range, for a given P_2 value, according to the analysis of Bower[42] for uniaxially oriented polymers.

Figure 13 shows the average P_2 values of the two characteristic polyene Raman bands measured with 180° scattering geometry. These P_2 values were calculated assuming either a cylindrical tensor or a molecular scattering tensor with only the a_{33} component being nonzero. Some representative P_2 results obtained with

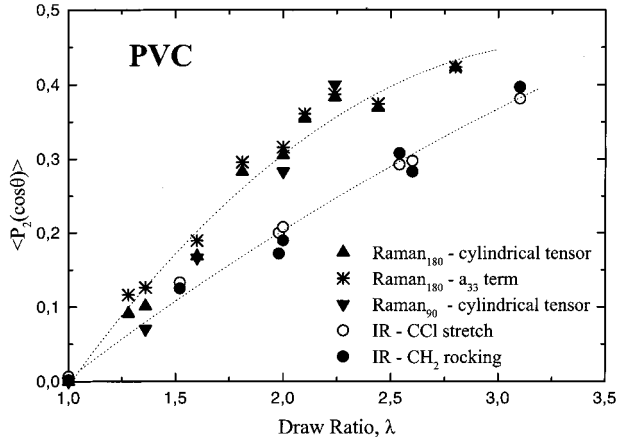

Figure 13. Second moment, P_2, of the orientation distribution function of industrial PVC samples vs draw ratio: (▲) Raman polyene average from 180° scattering assuming cylindrical tensor; (∗) Raman polyene average from 180° scattering assuming a tensor with only the a_{33} component being nonzero; (▼) Raman polyene average from 90° scattering assuming cylindrical tensor; (○) FTIR C−Cl stretch orientation average from the $\langle P_2(\cos\theta)\rangle$ data of the 613 and 639 cm^{-1} peaks; (●) FTIR 960 cm^{-1} band of CH_2 rocking. Lines are drawn to guide the eye.

the 90° scattering configuration and the assumption of a cylindrical tensor are included also in Figure 13. Comparison with the averaged infrared data on the C−Cl stretching modes at 613 and 639 cm^{-1} and CH_2 rocking mode at 960 cm^{-1} shows good agreement with respect to absolute values and the observed trends. Some differences between the Raman and FTIR P_2 values, which at $\lambda > 1.5$ amount up to an average of ca. 25%, can be attributed to a number of reasons. First, the two techniques probe different characteristics of the polymeric chain, with corresponding differences in sensitivity to various experimental and drawing parameters. In particular, Raman scattering is caused by polarizability fluctuations while FTIR absorption results from dipole moment fluctuations of the vibrating entity. Second, the Raman probe bands at 1515 and 1127 cm^{-1} reflect the orientation behavior of polyene sequences within the backbone of PVC chains, while the FTIR probes of the C−Cl stretching and CH_2 rocking modes most probably indicate orientation of short syndiotactic PVC segments. Therefore, the observed P_2 differences between infrared and Raman can most probably be accounted for by the different nature of the probed units and, in particular, by the greater length exhibited by the polyene sequences. To treat the case of a chain with more than one type of statistical segments, Shindo et al.[46] have generalized the Kuhn-Grün derivation[74] for the orientation of a segment in a uniaxially stretched rubber network. They were able to show that the degree of orientation is not the same for all segments, but it increases for larger segmental lengths. Therefore, the orientation information obtained in this work by the Raman and infrared techniques, although considering different segments of the macromolecular chains, seems to be comparable and well justified.

On that account, we may fairly reliably interpret the molecular orientation of conjugated double bond segments in terms of amorphous-like chain orientation in PVC. This indirect method for evaluating the degree of orientation might be useful for other polymers as well. A resonant Raman-active agent and/or highly anisotropic rigid rod guest−polymeric substance incorporated

into a host−polymer can be easily detected at low concentration levels and be used as an indicator of the molecular orientation of the processed host−polymer itself. Provided that the probe molecular structure is sufficiently different from that of the host−polymer itself, the guest should reside in the amorphous phase of the host and act as indicator of orientation of the host chains within this phase. Resonance Raman active polyene probes have been already incorporated through solvent[75] or melt mixing[65] techniques into polyethylene and used as indicators of molecular orientation in its amorphous phase.

In this work, we have found also that the Raman CH_2 bending mode at 1432 cm^{-1} is not so sensitive to molecular orientation. This might be tentatively accounted for by either the randomlike directionality of the corresponding polarizability ellipsoid relative to the chain axis and/or by a CH_2 normal mode coupling that depolarizes the corresponding scattered Raman photons. One way or another, the intensity of this band can play the role of an internal standard of PVC. We may anticipate that analogous CH_2 bending modes would present a similar behavior with respect to molecular orientation in other vinyl and vinylidene polymers as well. The insensitivity of the CH_2 bending mode may be combined with the high sensitivity of the polyene Raman bands and be used for the development of a new method for a fast and reliable evaluation of molecular orientation in drawn polymers. For this purpose, one can construct a calibration curve of P_2 vs the ratio of intensities I_{1515}/I_{1432} measured at selected polarization geometry. Using such a calibration curve, one can determine P_2 of a specimen stretched at an unknown draw ratio by measuring at the specific geometry one Raman spectrum and calculating the ratio I_{1515}/I_{1432}. When this method is combined with a flexible Raman probe[76] for accumulating polarized spectra, one may be able to monitor on-line and continuously the degree of molecular orientation in industrial processes of drawn vinyl and vinylidene polymers. The application of such a method to poly(vinyl chloride), poly(vinyl acetate), polyprolylene, polyethylene, and poly(vinylidene fluoride) is underway and results will be reported in a subsequent publication.

V. Concluding Remarks

Polarized resonance Raman microscopy and FTIR specular reflectance techniques have been employed to determine the degree of molecular orientation in uniaxially stretched industrial PVC samples. We have taken advantage of the partial thermal degradation of industrial PVC samples to polyenes and conditions for achieving resonance Raman enhancement of polyene modes at 1127 and 1515 cm^{-1}, to evaluate molecular orientation in the amorphous-like phase of drawn PVC. These Raman orientation data were found to show good agreement with corresponding infrared data for the C−Cl stretching modes deconvoluted at 613 and 639 cm^{-1} and the CH_2 rocking mode at 960 cm^{-1}. On the contrary, the CH_2 bending mode active in the Raman spectrum at 1432 cm^{-1} was found to be insensitive to the drawing process. In this context, a new Raman method was proposed for the fast, on-line evaluation of molecular orientation in uniaxially drawn vinyl and vinylidene polymers. A note is made of the fact that the resonantly enhanced Raman polyene bands are very sensitive to molecular orientation. The use of such bands reduces greatly the errors associated with tedious processes of deconvoluting infrared and Raman profiles, as well as with processes for determining the fourth moment of the distribution function of molecular orientation.

Acknowledgment. The authors would like to thank Mr. J. Charaktinos, Mr. I. Kolokouris, and Mr. V. Dikis of the research division of A. G. Petzetakis S. A. for making available the drawn PVC specimens. E.I.K. and G.D.C. gratefully acknowledge the valuable help of Mr. A. Patsis and Mr. Y. Yiannopoulos with FTIR measurements. Part of this work was supported by the Greek General Secretariat of Research and Technology in the framework of STRIDE−061, YPER-375 and AXIA-11 programs, by A. G. Petzetakis S. A., and by NATO's Scientific Affairs Division through the Science for Stability program.

References and Notes

(1) (a) *Developments in Oriented Polymers-1*; Ward, I. M., Ed.; Applied Science: London, 1982. (b) *Developments in Oriented Polymers-2*; Ward, I. M., Ed.; Elsevier Applied Science: London, 1987. (c) *Structure and Properties of Oriented Polymers*; Ward, I. M., Ed.; Chapman & Hall: London, 1997.
(2) Purvis, J.; Bower, D. I.; Ward, I. M. *Polymer* **1973**, *14*, 398.
(3) Purvis, J.; Bower, D. I. *Polymer* **1974**, *15*, 645.
(4) Satija, S. K.; Wang, C. H. *J. Chem. Phys.* **1978**, *69*, 2739.
(5) Jasse, B.; Koenig, J. L. *J. Polym. Sci., Polym. Phys. Ed.* **1978**, *16*, 2115.
(6) Maxfield, J.; Stein, R. S.; Chen, M. C. *J. Polym. Sci., Polym. Phys. Ed.* **1978**, *16*, 37.
(7) Zabel, K.; Schlotter, N. E.; Rabolt, J. F. *Macromolecules* **1983**, *16*, 446.
(8) Lauchlan, L.; Rabolt, J. F. *Macromolecules* **1986**, *19*, 1049.
(9) Pigeon, M.; Prud'homme, R. E.; Pezolet, M. *Macromolecules* **1991**, *24*, 5687.
(10) Gustafsson, G.; Inganas, O.; Osterholm, H.; Laakso, J. *Polymer* **1991**, *32*, 1574.
(11) Archer, L. A.; Fuller, G. G.; Nunnelley, L. *Polymer* **1992**, *33*, 3574; Archer, L. A.; Fuller, G. G. *Macromolecules* **1994**, *27*, 4359.
(12) Lafrance C.−P.; Chabot, P.; Pigeon, M.; Prud'homme, R. E.; Pezolet, M. *Polymer* **1993**, *34*, 5029.
(13) Jasse, B.; Tassin, J. F.; Monnerie, L. *Prog. Colloid Polym. Sci.* **1993**, *92*, 8. Kaito, A.; Kyotani, M.; Nakayama, K. *J. Polym. Sci., B: Polym. Phys.* **1993**, *31*, 1099.
(14) Kaito, A.; Nakayama, K.; Kyotani, M. *J. Polym. Sci., B: Polym. Phys.* **1993**, *29*, 1321.
(15) Li, W.; Prud'homme, R. E. *Polymer* **1994**, *35*, 3260; Abtal, E.; Prud'homme, R. E. *Polymer* **1993**, *34*, 4661.
(16) Lafrance C.−P.; Prud'homme, R. E. *Polymer* **1994**, *35*, 3927.
(17) Buffeteau, T.; Desbat, B.; Besbes, S.; Nafati, M.; Bokobza, L. *Polymer* **1994**, *35*, 2538.
(18) Citra, M. J.; Chase, B.; Ikeda, R. M.; Gardner, K. H. *Macromolecules* **1995**, *28*, 4007.
(19) Voyiatzis, G.; Petekidis, G.; Vlassopoulos, D.; Kamitsos, E. I.; Bruggeman, A. *Macromolecules* **1996**, *29*, 2244.
(20) Liao, M.-Y.; Rutledge, G. C. *Macromolecules* **1997**, *30*, 7546.
(21) Andrikopoulos, K.; Vlassopoulos, D.; Voyiatzis, G. A.; Yiannopoulos, Y. D.; Kamitsos, E. I. *Macromolecules* **1998**, *31*, 5465.
(22) Cole, K. C.; Ben Daly, H.; Sanschagrin, Nguyen, K. T.; Ajji, A. *Polymer* **1999**, *40*, 3505.
(23) Roe, R.-J. *J. Appl. Phys.* **1965**, *36*, 2024. Roe, R.-J. *J. Polym. Sci. A-2* **1970**, *8*, 1187.
(24) Bower, D. I. *J. Polym. Sci., Polym. Phys. Ed.* **1972**, *10*, 2135.
(25) Schlotter, N. E. In *Encyclopedia of Polymer Science and Engineering;* 2nd ed.; Mark, H. F., Bikales, N., Ovenberger, C. G., Megnes, G., Eds; Wiley: New York, 1988.
(26) Koenig, J. L. *Spectroscopy of Polymers*; ACS Professional Reference Book: American Chemical Society: Washington, DC, 1992; Chapter 3 and references therein.
(27) Jasse, B.; Koenig. J. L. *J. Macromol. Sci. C* **1979**, *17*, 61; *J. Polym. Sci., Polym. Phys. Ed.* **1980**, *25*, 1505.
(28) Purvis, J.; Bower, D. I. *J. Polym. Sci., Polym. Phys. Ed.* **1976**, *14*, 1461; Robinson, M. E. R.; Bower, D. I.; Maddams, W. F. *J. Polym. Sci., Polym. Phys. Ed.* **1978**, *16*, 2115.

(29) Robinson, M. E. R.; Bower, D. I.; Maddams, W. F. *Polymer* **1978**, *19*, 773.
(30) Rubčić, A.; Zerbi, G. *Macromolecules* **1974**, *7*, 754.
(31) Rubčić, A.; Zerbi, G. *Macromolecules* **1974**, *7*, 759.
(32) *Degradation and Stabilisation of PVC*; Owen, E. D., Ed.; Elsevier Applied Science Publishers Ltd,: London, 1984.
(33) Liebman, S. A.; Foltz, C. R.; Reuwer, J. F.; Obremski, R. J. *Macromolecules* **1971**, *4*, 134. Liebman, S. A.; Ahlstrom, D. H.; Quinn, E. J.; Geigley, A. G.; Meluskey, J. T. *J. Polym. Sci., Part A-1* **1971**, *9*, 1921.
(34) Gerrard, D. L.; Maddams, W. F. *Macromolecules*: (a) **1975**, *8*, 54; (b) **1977**, *10*, 1221; (c) **1981**, *14*, 1356.
(35) Baruya, A.; Gerrard, D. L.; Maddams, W. F. *Macromolecules* **1983**, *16*, 578.
(36) Martinez, G.; Mijangas, G.; Millan, J. L.; Gerrard, D. L.; Maddams, W. F. *Makromol. Chem*. **1984**, *185*, 1277.
(37) Cuthbertson, M. J.; Bowley, H. J.; Gerrard, D. L.; Maddams, W. F.; Shapiro, J. S. *Makromol. Chem*. **1987**, *188*, 2801.
(38) Bowley, H. J.; Gerrard, D. L.; Biggin, I. S. *Polym. Degrad. Stabil.* **1988**, *20*, 257.
(39) Williams, K. P. J.; Gerrard, D. L. *Eur. Polym. J*. **1990**, *26*, 1355.
(40) Bowden, M.; Donaldson, P.; Gardiner, D. J.; Birnie, J.; Gerrard, D. L. *Anal. Chem*. **1991**, *63*, 2915.
(41) Kip, B. J.; van Aaken, S. M.; Meier, R. J.; Williams, K. P. J.; Gerrard, D. L. *Macromolecules* **1992**, *25*, 4290.
(42) Hillemans, J. P. H. M.; Colemonts, C. M. C. J.; Meier, R. J.; Kip, B. J. *Polym. Degrad. Stabil.* **1993**, *42*, 323.
(43) Bowden, M.; Brandley, J. W.; Dix, L. R.; Gardiner, D. J.; Dixon, N. M.; Gerrard, D. L. *Polymer* **1994**, *35*, 1654.
(44) Brandley, J. W.; Dix, L. R.; Gardiner, D. J.; Dixon, N. M.; Gerrard, D. L. *Polymer* **1996**, *37*, 205.
(45) Remillard, J. T.; Jones, J. R.; Poindexter, B. D.; Helms, J. H.; Weber, W. H. *Appl. Spectrosc.* **1998**, *52*, 1369.
(46) Shindo, Y.; Read, B. E.; Stein, R. S. *Makromol. Chem*. **1968**, *118*, 272.
(47) Everall, N. J.; Bibby, A. *Appl. Spectrosc.* **1997**, *51*, 1083.
(48) Hobbs, J. P.; Sung, C. S. P.; Krishnan, K.; Hill, S. *Macromolecules* **1983**, *16*, 193. Gupta, M. K.; Carlson, D. J.; Wiles, D. M. *J. Polym. Sci., Polym. Phys. Ed.* **1984**, *22*, 1011. Mirabella, F. M., Jr. *J. Polym. Sci., Polym. Phys. Ed*. **1984**, *22*, 1283, 1293.
(49) Pirnia, A.; Sung, C. S. P. *Macromolecules* **1988**, *21*, 2699.
(50) Kaito, A.; Nakayama, K.; Kanetsuna, H. *J. Polym. Sci., Polym. Phys. Ed*. **1988**, *26*, 1439. Kaito, A.; Nakayama, K.; Kyotani, M. *J. Polym. Sci., Polym. Phys. Ed*. **1991**, *29*, 1321. Kaito, A.; Nakayama, K. *Macromolecules* **1992**, *25*, 4882. Kaito, A.; Kyotani, M.; Nakayama, K. *J. Polym. Sci., Polym. Phys. Ed*. **1993**, *31*, 1099.
(51) Jansen, J. A. J.; van der Maas, J. H.; de Boer, A. P. *Macromolecules* **1991**, *24*, 4278.
(52) Cole, K. C.; Guevremont, J.; Dumoulin, M. M. *Appl. Spectrosc.* **1994**, *48*, 1513.
(53) Everall, N. J.; Chalmers, J. M.; Local, A.; Allen, S. *Vibr. Spectrosc.* **1996**, *10*, 253.
(54) Clayden, N. J.; Eaves, J. G.; Croot, L. *Polymer* **1997**, *38*, 159.
(55) Kaito, A.; Kyotani, M.; Nakayama, K. *Macromolecules* **1991**, *24*, 3244.
(56) (a) Kamitsos, E. I.; Patsis, A. P.; Karakassides, M. A.; Chryssikos, G. D. *J. Non-Cryst. Solids* **1990**, *126*, 52. (b) Varsamis, C. P.; Kamitsos, E. I.; Machida, N.; Minami, T. *J. Phys. Chem. B* **1997**, *101*, 3734.
(57) Bower, D. I. *J. Polym. Sci., Polym. Phys. Ed*. **1981**, *19*, 93.
(58) Fraser, R. D. B. *J. Chem. Phys.* **1953**, *21*, 1511; **1956**, *24*, 89.
(59) Stein, R. S. *J. Polym. Sci.* **1958**, *31*, 335.
(60) Krimm, S. *J. Polym. Sci.* **1964**, *C7*, 3.
(61) Kürti, J.; Kuzmany, H. *Phys. Rev. B* **1991**, *44*, 597. Zannoni, G.; Zerbi, G, *J. Mol. Struct.* **1983**, *100*, 505.
(62) Parker, S. F.; Tavender, S. M.; Dixon, N. M.; Herman, H.; Williams, K. P. J.; Maddams, W. F. *Appl. Spectrosc.* **1999**, *53*, 86.
(63) Gussoni, M.; Castiglioni, C.; Zerbi, G. In *Spectroscopy of Advanced Materials*; Clark, R. J. H., Hester, R. E., Ed.; John Wiley & Sons Ltd.: London, 1991**;** Chapter 5 and references therein.
(64) Mead, D. W. Personal communication, 1996.
(65) Everall, N.; Chalmers, J.; Mills, P. *Appl. Spectrosc.* **1996**, *50*, 1229.
(66) Tasumi, M.; Shimanouchi, T. *Spectrochim. Acta* **1961**, *17*, 731.
(67) Pohl, H. U.; Hummel, D. O. *Makromol. Chem*. **1968**, *113*, 190, 203.
(68) Theodorou, M.; Jasse, B. *J. Polym. Sci., Polym. Phys. Ed*. **1986**, *24*, 2643.
(69) Jabarin, S. A. *Polym. Eng. Sci.* **1991**, *31*, 638.
(70) Karacan, I.; Bower, D. I.; Ward, I. M. *Polymer* **1994**, *35*, 3411.
(71) Tasumi, M.; Shimanouchi, T. *Polymer* **1971**, *2*, 62.
(72) Bower, D. I.; King, J.; Maddams, W. F. *J. Macromol. Sci. Phys.* **1981**, *B20*, 305.
(73) Jakson, R. S.; Bower, D. I.; Maddams, W. F. *J. Polym. Sci., Polym. Phys. Ed*. **1990**, *28*, 837.
(74) Kuhn, W.; Grun, F. *Kolloid-Z.* **1942**, *101*, 248; Treloar, L. R. G. *Trans. Faraday Soc.* **1954**, *50*, 881.
(75) Margulies, L.; Stockburger, M. *J. Raman Spectrosc.* **1979**, *8*, 26.
(76) Lewis, I. R.; Griffiths, P. R. *Appl. Spectrosc.* **1996**, *50*, 12A.

MA991772M